

Photochemical Sensing of Semicrystalline Morphology in Polymers: Pyrene in Polyethylene

M. R. Vigil, J. Bravo, T. D. Z. Atvars,[†] and J. Baselga*

E. P. Superior, Universidad Carlos III de Madrid, 28911 Leganés, Spain

Received January 28, 1997; Revised Manuscript Received May 21, 1997[®]

ABSTRACT: Pyrene was inserted into a low-density polyethylene matrix. Fluorescence spectra as a function of temperature and the differential scanning calorimetry (DSC) trace were recorded simultaneously. Along with the usual vibronic bands, a low-intensity band at 365 nm appears at higher energies with respect to the 0–0 transition in the pyrene fluorescence spectra. The fluorescence intensity of this small band increased with temperature, and an isoemissive point was observed to occur at 368 nm. This emission was interpreted as arising from pyrene molecules located in the outer rigid interfacial region of polymer crystallites. Its temperature-dependent fluorescence was interpreted in terms of electron–phonon coupling; two phonons which coincide with fundamental vibrations of polyethylene were necessary to fit experimental data. Coupling with a high-energy phonon was possible at low temperature, whereas, above the β relaxation temperature, phonon coupling occurs with a lower-energy phonon. The α relaxation was detected as a maximum in fluorescence intensity since above its characteristic temperature, nonradiative processes begin to operate.

I. Introduction

Luminescent techniques have long been employed in biological systems.¹ However, only recently have these techniques begun to be considered as customary tools in synthetic polymer research.^{2,3} The main benefits of using molecular fluorescent probes and labels are the multiple interactions that may occur between excited states and their environment. Using an adequate probe selection and insertion procedure, different research topics of current interest can be approached: polymer miscibility,⁴ conformational dynamics in solution,^{5–7} diffusion in polymers,⁸ surface characterization,⁹ polymer relaxation processes,^{10,11} and monitoring of polymerization reactions.^{12,13} Another important experimental advantage is that fluorescent probes can be incorporated either intrinsically or extrinsically with very low concentration and fluorescence can be detected with very high sensitivity.

Secondary relaxation processes of polyethylene (PE), although extensively studied, are not fully understood because of the morphological and microstructural complexity of this polymer.^{14,15} Using anthracene luminescence,¹⁶ one of the authors observed that the change of fluorescence intensity with temperature parallels the three main relaxations reported for polyethylene. Since this molecular probe was not located inside the crystalline region, fluorescent intensity changes were interpreted as due to relaxations in the amorphous bulk polymer and at the crystallite interfaces. In fact, it is currently thought that the interfacial crystalline structure is coupled with the motion within the crystallite interior.¹⁴ Location of fluorescence probes at the crystallite interfaces may prove to be a powerful tool for studying such kind of coupled crystallite and interfacial relaxation processes. In addition, because of the different time and length scales in which thermal, dynamic mechanical, and fluorescence phenomena may occur, all of them may give complementary information to provide further insights into polymer relaxation phenomena.

One of the major problems in comparing results on polymer relaxation processes obtained from different techniques, lies in the difficulty of working with the same sample, with the same thermal history, and in the same experimental conditions. The aim of this work is to report fluorescence measurements of pyrene-doped polyethylene in the temperature range in which the α and β relaxations and melting transition are reported to occur and to employ a new technique which combines fluorimetry and calorimetry in such a way that differential scanning calorimetry (DSC) traces and fluorescence spectra can be recorded simultaneously. The main advantage of this procedure is that we can perform both measurements with the same sample, with the same thermal history, and at the same time.

In this work we selected pyrene as a fluorescent probe for several reasons, including a set of well-known photophysical properties: long lifetime, fluorescence emission with a very well resolved vibrational structure, high monomer and excimer quantum yields, and strong environmental effects upon the fluorescence emission.¹⁷ Pyrene, which belongs to the D_{2h} point group, has four singlet states which are as follows,¹⁸ in order of increasing energy: L_b (S_1 , ~ 370 nm), L_a (S_2 , ~ 337 nm), B_b (~ 274 nm), and B_a (~ 244 nm) (the first and third states are of B_{1u} symmetry and the other two states of B_{2u} symmetry). The four states are electric dipole allowed for one photon transition from the ground state, but transition into the L_b , which is y -polarized, has a very small transition moment;¹⁸ therefore, pyrene is usually excited into the L_a state.

The 0–0 fluorescence transition of pyrene in n -heptane pseudo-monocrystal at 8 K¹⁹ and other frozen Shpol'skii matrices appears at $26\,926\text{ cm}^{-1}$ (371.4 nm).²⁰ In these matrices, the fluorescence spectrum consists of sharp vibronic lines produced by a vibronic mechanism resulting from the Herzberg–Teller and Born–Oppenheimer coupling terms. The fluorescence bands are found to be highly temperature-dependent;¹⁹ also, high-energy multiplets occur when Shpol'skii solutions are quick frozen. The observed band broadening (observed also in our experiments with pyrene in polyethylene) was associated with a not too well-structured medium (i.e., not well-crystallized medium); it has been also suggested that electron–phonon coupling may

* To whom correspondence should be addressed.

[†] Permanent address: Instituto de Química, Universidade Estadual de Campinas, Caixa Postal 6154, Campinas, CEP 13083-970, SP, Brazil.

[®] Abstract published in *Advance ACS Abstracts*, July 15, 1997.

explain the strong temperature dependence of the fluorescent band intensities.

The strength of the 0–0 transition of the pyrene molecule depends on the vibronic coupling between the electronic states S_1 and S_2 through b_{3g} Raman active vibrational modes ($E(S_1) - E(S_2) \approx 3000 \text{ cm}^{-1}$).¹⁷ Pyrene has at least four b_{3g} normal modes in the frequency range $1100\text{--}1500 \text{ cm}^{-1}$ that can participate in the coupling, with the dominant at 1100 cm^{-1} ; the vibrational distortions of the nuclear coordinates with this symmetry generates an induced dipole moment responsible for the solvent–solute interaction or Ham effect. Other vibrational band intensities depend on the difference between the Herzberg–Teller and Born–Oppenheimer vibronic contributions. These differences between the coupling mechanisms in different vibrational bands can explain the solvent polarity dependence of the vibronic I/III ratios,²¹ i.e. the polarity py-scale.^{17,21,22}

Although there is a large amount of experimental data available for pyrene emission in different media, very few works have been reported describing the dependence of the vibronic structure upon a large temperature range. In this work we discuss some aspects related to the dependence of the pyrene vibrational structure on temperature in the range from -100 to 150°C and in a polyethylene matrix.

II. Experimental Section

Commercial low-density polyethylene sheets of 4 mm thickness were employed in this work as starting materials. Films of about 0.4 mm were prepared by pressing PE sheets at 110°C for 30 min and cooling down to room temperature for a period of 2 h. Slices of about 20 mm (wide) \times 80 mm (length) and \times 0.4 mm (thick) were cut and immersed in chloroform for 4 h for surface cleaning. Afterward they were vacuum dried at 50°C for 3 h. The clean specimens were immersed in an *n*-heptane–pyrene solution (10^{-3} M) for a period of 2 h, in order to allow the probe to diffuse into the polymer sample; the sample's surface was washed with *n*-heptane to remove any remaining pyrene on the surface, and finally, the solvent was removed by extensive vacuum drying for a week. The molar concentration of pyrene in the polymer matrix, being determined by UV spectrometry and using the extinction coefficient of cyclohexane solutions,¹⁶ was $2 \times 10^{-4} \text{ M}$.

Calorimetric measurements were performed on a Perkin-Elmer DSC-7, at $2^\circ\text{C}/\text{min}$, in the temperature range -100 to 150°C . The sample was inserted in the calorimeter at low temperature (-100°C) and was allowed to thermalize for 30 min under N_2 . Steady state fluorescence measurements were simultaneously performed using a Perkin-Elmer LS-50B fluorimeter. The excitation wavelength was set at 333 nm, and emission spectra were recorded from 350 to 500 nm; the scan rate was selected to record each spectrum every 5.5°C . Bandwidth slits for excitation and emission were 5 and 3 nm, respectively. Excitation spectra of the samples were performed at room temperature and at different emission wavelengths ranging from 295 to 480 nm. Details of the optical arrangement for the coupling of the two instruments can be found elsewhere.¹² The first DSC trace obtained for this sample is shown in Figure 1. It can be observed that the only transition which is clearly resolved is the melting process; neither the β relaxation nor the α relaxation can be observed. This behavior is typical in the first scan of low-density polyethylene. Subsequent scans erase the thermal history of the polymer and are not very advisable when trying to characterize industrial polymers.

III. Results

3.1. Emission Spectra: General Temperature Effects. In Figure 2 the fluorescence spectra of pyrene in the polyethylene matrix are shown for several tem-

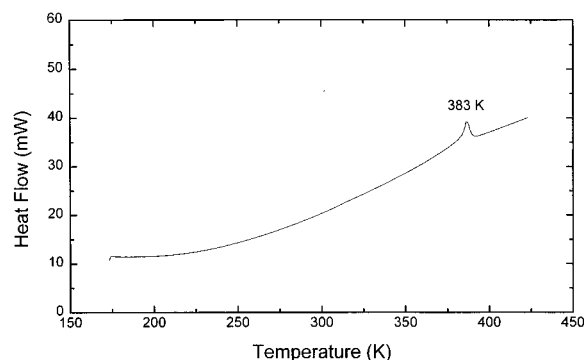


Figure 1. DSC trace of the low-density polyethylene sample, run at 2 K min^{-1} .

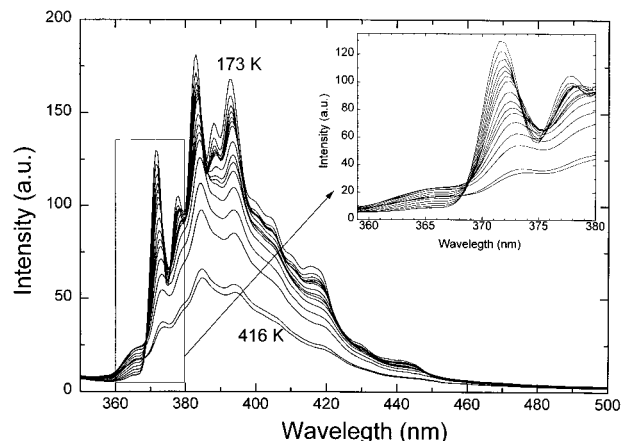


Figure 2. Fluorescence emission spectra of pyrene in low-density polyethylene at several temperatures, obtained during a heating cycle at a rate of $2^\circ\text{C}/\text{min}$. The insert expands the wavelength region in which an isoemissive point is observed.

peratures during the heating program. Pyrene emission at low temperature shows a fluorescence band centered at 390 nm whose intensity decreases with temperature. Up to sixteen vibronic bands have been reported for pyrene¹⁷ at very low temperatures, but only the five most intense vibronic bands are resolved here. The vibronic band centered at 372 nm is assigned to the *zero-phonon* band;^{17,22,23} in the terminology of Kalyanasundaram and Thomas,¹⁷ this band is termed as I band; the other predominant bands are sequentially numbered from II to V. Band III has been assigned to a $S_{1,v=0} \rightarrow S_{0,v=1}$ transition.²¹

Figure 2 shows a very weak band at energies higher than the zero-phonon band centered at about 365 nm and whose intensity increases with temperature. This band appears in all of our samples; a careful analysis of all the available literature reveals that it also appears in all the examined pyrene spectra,^{17,21,22} but, to the best of our knowledge, it has not been assigned yet. At about 368 nm, an isoemissive point can be observed; this point will be discussed later.

In the wavelength range at which excimer fluorescence usually appears (around 480 nm) a very small increase of fluorescence intensity can be observed, but since the pyrene concentration is low, the excimer contribution does not appear to be significant. It is noteworthy that the fluorescence quantum yield for pyrene excimer fluorescence is much higher than for the monomer,²⁴ which means that, in our samples, the monomer concentration is much higher than that of the excimer.

Other observations on figure 2 are as follows: (i) the vibrational monomeric fluorescence peaks shift gradu-

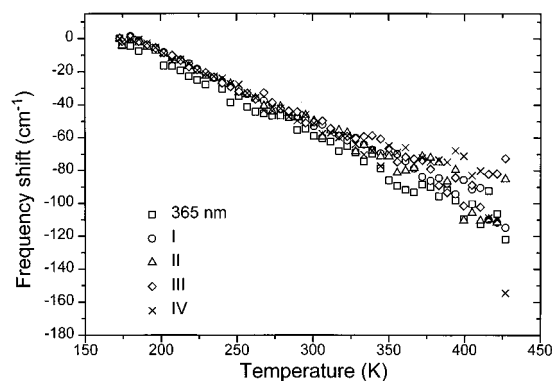


Figure 3. Frequency shift of fluorescence emission maxima as a function of temperature.

ally to lower energies on heating; (ii) the bandwidth of the different vibronic bands increases with temperature. The first effect is analyzed in Figure 3, in which the peak shift for some vibronic fluorescent bands is plotted against temperature. Peak positions were obtained by curve fitting, converting the wavelength scale to wave-number scale using standard procedures.¹ The shift has been defined as the difference between the energy of the vibronic transition at the lowest temperature and at the current temperature. Linear plots with negative slopes are obtained in every case. The slopes range from $-0.446 \pm 0.006 \text{ cm}^{-1} \text{ K}^{-1}$ for the emission band at 365 nm to -0.38 ± 0.01 for III band.

Temperature-dependent peak shifts for absorption processes of nonpolar molecules in nonpolar solvents (such as pyrene in polyethylene) are usually interpreted as arising from a balance between two opposing effects:²⁵ (a) as the temperature is raised, the population of certain vibronic levels may be perturbed, changing the band shape of the transition and shifting it through lower energies; (b) at the same time, the solvent density can decrease, resulting in a shift to higher energies because the stabilizing effect of dispersion forces (induced dipole–induced dipole energy) also decreases. For emission processes the same predictions may operate.

A well-known example where density effects operate is azulene in pentane;²⁵ a linear frequency shift with solvent density has been found for the 1B_b absorption transition, the magnitude of which is about -110 cm^{-1} per 10% of the solvent density increase. For low-density polyethylene, it is expected that density could decrease about 12% in the temperature range covered in this work; therefore, the associated frequency blue shifts should be about the same order of magnitude. However, as can be seen in Figure 3, shifts toward lower energies are found: about $+70 \text{ cm}^{-1}$ for the III band, $+120 \text{ cm}^{-1}$ for the band at 365 nm, and about $+155 \text{ cm}^{-1}$ for the IV band. Although some important matrix relaxations occur, with an associated density variation within the temperature range mentioned above, the peak shifts in pyrene do not reflect them. Therefore, we must conclude that, in this system, band shape variations predominate over dispersion forces variations, and this is in line with the band broadening mentioned above.

3.2. Excitation Spectra. To study the properties of the high-energy band at 365 nm, the room temperature excitation spectrum at 365 nm is compared in Figure 4 with excitation spectra collected at four characteristic pyrene emission wavelengths: I, II, III, and V; in addition, excitation spectra at the usual excimer emission wavelength (480 nm) is included, and all of them are corrected for the base line and normalized to the maximum at 337.5 nm.

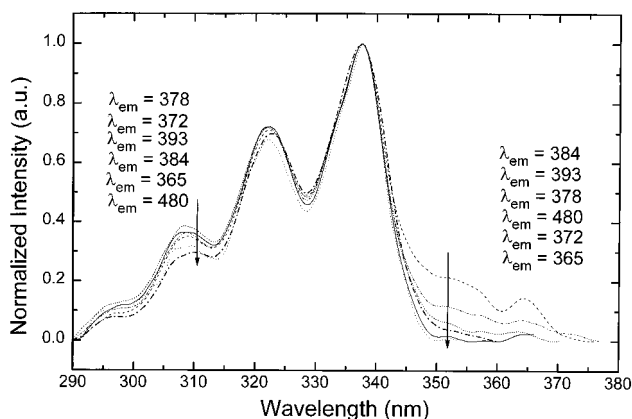


Figure 4. Excitation spectra collected at four characteristic pyrene emission wavelengths (I, II, III, and V) and at the usual excimer emission wavelength (480 nm). Spectra are corrected for the base line and normalized to the maximum at 337.5 nm.

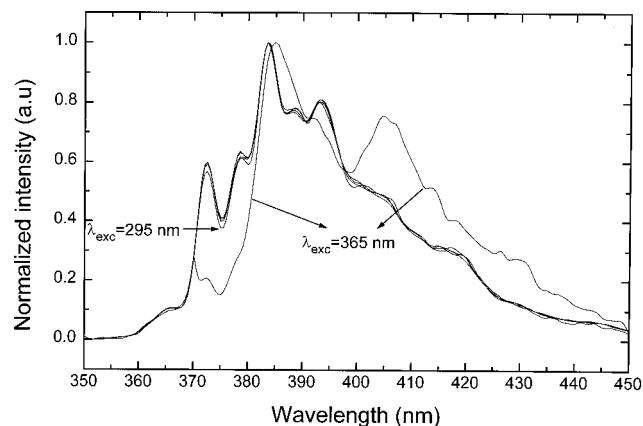


Figure 5. Room temperature fluorescence emission of pyrene in polyethylene at the following excitation wavelengths: 295, 309, 322, 337, and 365 nm.

The vibronic bands that appear in the wavelength range 290–350 nm correspond to the second excited singlet absorption, and a general good coincidence of the spectra is observed, regardless of the emission wavelength. This result indicates that the species emitting at 365 nm and at the other characteristic emission wavelengths of pyrene are the same; therefore the presence of impurities can be ruled out.

However, slight differences can be found in both the high- and low-energy regions of the excitation spectra. In the wavelength range 350–375 nm, the very weak vibronic bands correspond to the first singlet absorption region ($S_0 \rightarrow S_1$). At about 365 nm a vibronic absorption band is observed which coincides with the emission band observed in Figure 2. Since the excitation spectra have been normalized at 337.5 nm, the relative intensity variations of the 365 absorption band can be compared; it seems that the highest intensity corresponds to an emission wavelength of 384 nm. More detailed analysis was made by recording the room temperature emission spectrum for an excitation wavelength of 365 nm and comparing it with emission spectra at other excitation wavelengths. These are presented in Figure 5. A dramatic change in the shape of the spectrum is observed. The main differences found are as follows: (a) the III band, for which the maximum fluorescence intensity is observed (in accordance with the excitation spectrum observation), appears shifted toward lower energies by about 2 nm with respect to the III band of the normal spectrum of pyrene; (b) the width of the III

band appears to be increased, suggesting that the contribution of the IV band (or other vibronic bands) is enhanced (this enhancement may also explain the red shift in band III); (c) the fluorescence from low-energy vibronic contributions also seems to be enhanced, specifically at 405 nm, which remains as only a shoulder in the normal pyrene emission spectrum; (d) the intensity of the I and II bands is greatly reduced (the III/I band ratio increases from 1.69 for 337.5 nm excitation (a typical value for nonpolar solvents such as polyethylene), to 4.9 for 365 nm excitation). All of these observations can be understood by taking into account that excitation at energies lower than second singlet absorption can inhibit vibronic coupling between S_1 and S_2 electronic states, which is responsible for the shape of the normal pyrene emission spectrum.²¹ Particularly, in the case of the intensity of the 0–0 transition induced by vibronic coupling, since it is determined exclusively by the Herzberg–Teller coupling between electronic states S_1 and S_2 , its intensity should be greatly decreased when excitation takes place at 365 nm.

In the high-energy region of the excitation spectra presented in Figure 4, some perturbations in the high-energy vibronic states can be observed. For the high-energy second singlet vibronic bands, the highest intensities are achieved when spectra are viewed at 372 and 378 nm and the lowest intensities when viewed at 365 and 480 nm. Using the method reported by Winnik,²⁶ the peak-to-valley intensity ratios ($I_{337.5}/I_{328.5}$) were calculated. There are no significative differences in these values, which are about 2.3 for spectra viewed at excimer emission wavelength and 2.0–2.3 for other monomer emission wavelengths. These values are in agreement with the ones reported for pyrene monomer emission measured in other environments²⁶ and confirm that excimer contribution is negligible.

IV. Discussion

Regardless of the fact that the band at 365 nm, whose existence has never been described in the literature, is blue shifted with respect to the 0–0 band, we attempt to explain its spectral origin considering the following possibilities: (i) solvent Raman band, (ii) dimer formation with pyrene molecules in a different sandwich geometry from the excimer, (iii) polarity effects, (iv) specific intramolecular vibronic coupling, and (v) electron–phonon coupling.

In Figure 5, pyrene emission spectra, corrected for the base line and normalized at the III band, are presented using five excitation wavelengths $\lambda_{\text{exc}} = 295, 309, 322, 337, \text{ and } 365 \text{ nm}$; the first four excitation wavelengths correspond to the vibrational structure of the S_2 electronic state. No significant variations in the band ratios are observed when excitation occurs at any of the different second singlet vibronic bands, although, as stated above, because small differences were obtained in the intensities of the high-energy bands of the excitation spectra, some variations in the overall fluorescent response may be observed. Neither wavelength shift nor fluorescent intensity change are obtained for the 365 emission band. Therefore it can be concluded that this band cannot be assigned to the solvent Raman vibrational mode.

Winnik²⁶ pointed out that some stable conformations of pyrene dimers could produce fluorescence emission at higher energies than excimer or the monomer emission, if the intermolecular distance between pyrene molecules was longer than 3 Å. Since these static

dimers have a stable structure, they have a bonding potential curve for both ground and electronic excited states. If we consider that they exhibit a parallel geometry, the exciton theory establishes that, for a certain population of pyrene dimers, the electronic transition splits into a band, the high-energy portion of which is allowed; therefore the electronic spectra should be shifted toward higher energies.²⁵ If these stable dimers with this geometry are present in our system and if they were responsible for the fluorescence emission at 365 nm, a relative enhancement of the 365 nm emission band should be expected when exciting at high energies; this was not observed in our experiments. Furthermore, in considering that this band has been observed in many other systems, including low-viscosity media, we conclude that the band at 365 nm cannot be assigned to the dimer forms of pyrene.

As pointed out before, the relative intensity of the emission vibrational bands depends on the vibronic coupling between S_1 and S_2 electronic excited states, and this coupling is strongly dependent on the polarity of the medium.²¹ Using the polarity py-scale we have obtained that polyethylene behaves like a nonpolar solvent, but, as also mentioned above, the 365 nm band is also observed in other media with very different polarities. Therefore, we cannot ascribe this band to a polarity effect on the electronic spectra.

However, since the relative intensities of the vibrational bands depend on the vibronic coupling between vibrational modes of both S_1 and S_2 electronic excited states, it should be considered that this coupling may produce at least two types of emissive pathways. In other words, the initial state for the 365 emission may differ from the initial state for the 0–0 emission.

Pyrene in a partially crystalline matrix is not predicted to be in a homogenous and isotropic medium. Some molecules may be randomly distributed in the amorphous region, but others may be located at the interface between the spherulite and amorphous regions, i.e. the strained amorphous regions. Two kinds of related effects may operate: straining and inefficient dielectric coupling.

Vibronic coupling between S_1 and S_2 states involves vibrational modes which simultaneously expand the long and short molecular axes.²¹ If the interface cavity in which some pyrene molecules are located imposes restrictions on excited pyrene geometry, the final state of the coupling may be quite different from coupling in a flexible environment. Moreover, during their excited state lifetime, pyrene molecules may induce a dipolar moment in the surrounding polymer segments, which results in some kind of dielectric coupling. Because of polymer rigidity, dielectric relaxation may not occur and the pyrene may emit from a high-energy unrelaxed state. Nevertheless, this effect should not be very important because the pyrene dipolar moment in the excited state, which is responsible for the dielectric coupling with the environment, is quite low. In any case, both effects should be more pronounced at temperatures at which the polymer mobility is low, yet quite the opposite is observed, suggesting that the initial state for the 365 nm emission band is not populated from higher energy levels.

Taking into account that the fluorescence intensity of the 365 nm band is temperature dependent (more intense at higher temperatures) and that an isoemissive point is obtained at 368 nm, we may conclude that both the 365 and 0–0 bands are linked by some kind of

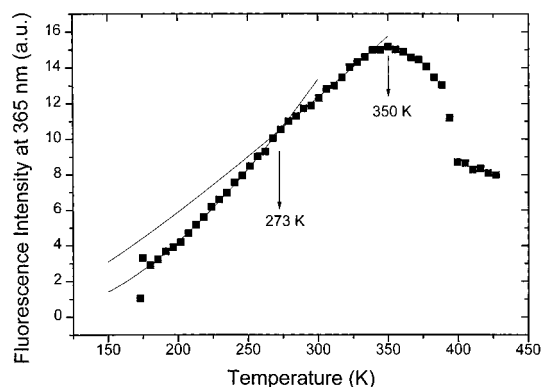


Figure 6. Integrated fluorescence intensity of the 365 band as a function of temperature. The lines represent the best fits to the Bose–Einstein function in the temperature ranges 180–273 and 273–350 K.

excited state equilibrium whereby the 365 band may be populated at the expense of the 0–0 transition. The 365 nm emission could be presumed to be a “hot band”, but hot bands usually deform the low-energy region of emission spectra because high-energy vibronic levels of the ground state become thermally populated; in our case, the 365 nm band appears in the high-energy region of the spectra. Alternatively, high-energy vibronic levels of the S_1 state may be thermally populated from the lowest vibronic level of the same S_1 state; but since internal conversion or vibrational relaxation occur in a time scale of tens of picoseconds,²⁷ emission from higher vibronic levels should not be expected. Finally, if emission at 365 nm were due to a hot band, that is to say, if it is an intrinsic pyrene process which occurs without cooperation from the solid environment, then the 365 nm band intensity should increase with temperature throughout the temperature range; this is not observed in Figure 2 and Figure 6. Therefore, since the initial state of the 365 emission is of a higher energy than the initial state of the 0–0 emission, the “extra” energy must be provided by the polymer matrix.

Pyrene has a large number of fundamental vibrations and harmonics associated with its different electronic states.²⁸ In the B_{1u} state, vibrations range between 498 and 3102 cm^{-1} . Polyethylene also has numerous vibrational modes. For an infinite isolated methylene chain in extended conformation, the optical branch of its dispersion curve^{29,30} shows two fundamental internal modes in the range 2848–2919 cm^{-1} and five fundamental lattice modes (wagging and rocking) in the range 721–1442 cm^{-1} which are active in IR or Raman. The vibrational spectra for a low-density polycrystalline polyethylene is rather more complicated because of coupling between different vibrational frequencies and because the number of atoms which may participate in the vibrations should depend on the temperature. Therefore there is a large number of phonons which may be coupled with the excited pyrene molecule.

Linear electron–phonon coupling may be a suitable hypothesis for explaining the appearance of the emission at 365 nm and its intriguing temperature dependence. The intensity of the emission process should be a linear function of the population of the initial state of the transition. As temperature is increased, the mean thermal occupancy of this high-energy vibronic state should increase and, consequently, fluorescence intensity should increase also. At temperature T , the average value of the number of phonons in a mode k , $\langle n_k \rangle$, which vibrates at frequency ω above the zero-point energy is

given by the Bose–Einstein factor:³¹

$$\langle n_k \rangle = \frac{1}{\exp\{\hbar\omega/kT\} - 1}$$

$$I_{365} \propto \langle n_k \rangle \quad (1)$$

If it is assumed, as a simplifying assumption, that the vibrational state of the matrix can be represented by only one mode,³¹ then eq 1 allows us to estimate the energy of the representative phonon of the coupled system since the number of photons emitted from the high-energy vibronic state should be proportional to the mean thermal occupancy.

In Figure 6, the fluorescence intensity at 365 nm is plotted against temperature. The lines represent the best fit of eq 1 in which ω was left as an adjustable parameter. As can be observed, it was not possible to fit the entire temperature range with a single phonon. In the low-temperature region, up to 273 K, a good fit was obtained for a phonon of $2810 \pm 35 \text{ cm}^{-1}$. In the high-temperature range, up to 350 K, a lower energy phonon of $1437 \pm 61 \text{ cm}^{-1}$ fits the temperature dependence of the fluorescence at 365 nm.

The fact that good fits were obtained in both regions may prove that the initial state for 365 emission populates thermally from the initial state of the 0–0 transition, and, therefore, electron–phonon coupling may be the mechanism which originates the 365 nm fluorescence response. A tentative explanation for the two temperature ranges may be found if we take into account that the β relaxation for polyethylene has been reported to occur^{14,32} at about 240–270 K. Therefore, it should be expected that below 273 K only high-energy internal vibrational modes of polyethylene chains may be sufficiently populated to be coupled with excited pyrene; therefore, a high-energy phonon should be expected. At temperatures above 273 K, because chain mobility increases, vibrational modes associated with segmental mobility, which are of lower energy as indicated in the polyethylene dispersion curve,^{29,30} should begin to be populated; therefore, a lower energy phonon should describe the vibration state of the system more adequately.

Finally, at temperatures above 355 K, depopulation of the high-energy vibronic state is observed because the increasing trend of the fluorescent intensity is reversed. The α relaxation is reported to occur^{14,32} in the temperature range between 355 K and melting; for this polymer sample it appears at 385 K (measured as the peak maximum in the DSC trace). It is usually assumed that this high-temperature relaxation results from the motion of chain units located within the crystalline portion of the polymer and that the outer part of the crystallites or interfacial region is coupled with the crystallite interior. With the insertion procedure employed in this work, the pyrene cannot be located inside the crystallites; therefore some pyrene molecules should be located at the crystallites interface, where their emission reflects the intracrystallite relaxation. This region should have some lattice character in order for vibrational coupling between pyrene and the matrix to be possible. This is consistent with the existence of a rigid amorphous fraction predicted from calorimetric measurements.³³ When α relaxation begins to operate, the lattice character of the interfacial region should decrease gradually until melting occurs; therefore, pyrene emission at 365 should decrease because phonon coupling is no longer maintained. At melting,

interfacial volume disappears and, therefore, emission by pyrene at 365 nm decreases abruptly.

Nevertheless, at the same temperature at which a maximum intensity is obtained, the isoemissive point disappears (Figure 2). Above 355 K, the equilibrium between the initial states for emission at 365 and at 372 nm is no longer maintained. This means that some new photophysical processes may begin to operate in this high-temperature range. If it is assumed that emission at 365 nm comes from pyrene molecules located in very rigid environments, at temperatures below 355 K, collisional quenching (as a source of nonradiative processes) is inhibited because pyrene molecules are not free for translation motion. When the interfacial region acquires some mobility, collisional quenching may begin to operate and nonradiative transitions may compete with radiative emission.

In comparing the energy of the phonons with the dispersion curve for polyethylene, there is a noteworthy match with some fundamental vibrations in the polymer. The phonon of $2810 \pm 35 \text{ cm}^{-1}$ coincides with two vibrations of polyethylene: 2848 (active in Raman) and 2851 (active in IR). We have confirmed experimentally that this IR active vibration mode is more populated at low temperature than at room temperature.³⁴ The lower energy phonon $1437 \pm 61 \text{ cm}^{-1}$ may also be ascribed to a Raman mode of polyethylene which takes place at 1440 cm^{-1} or to the IR active mode at 1463 cm^{-1} . Nevertheless, since the energy difference between the 0–0 and 365 emissions is about 550 cm^{-1} , the question as to the exact mechanism by which an excited pyrene molecule may absorb a phonon of energy much greater than 550 cm^{-1} but emit near the 0–0 transition remains open; about two-thirds to five-sixths of the phonon energy is lost in the process.

V. Conclusions

The small emission band at 365 nm found in the fluorescence spectra of pyrene in a polyethylene matrix seems to come from pyrene molecules located in a very rigid environment. Since the insertion procedure employed does not enable the probe to be introduced inside the crystallites, the crystallite interfacial region must be the host environment.

The temperature dependence of this high-energy emission band has been interpreted in terms of electron–phonon coupling. A single vibrational mode was not able to fit the entire temperature range since pyrene fluorescence senses the β relaxation, which appears for the samples employed in this work at 273 K. Below 273 K, phonon coupling occurs with high-energy phonons whose energy coincides with some fundamental internal polyethylene vibrations. Above 273 K, interfacial polyethylene extended chains acquire some mobility and the coupling with pyrene occurs with a lower energy phonon whose energy coincides with some lattice vibrations. At the α relaxation temperature, chain mobility is so increased that nonradiative processes begin to operate and the fluorescence intensity decreases.

Finally, it can be concluded that the photochemistry of fluorescent probes located in selected host environments is a powerful technique for studying the morphology of semicrystalline polymers.

Acknowledgment. J. Baselga thanks CAM and CICYT (Projects No. 247/92 and MAT 93-0823) for financial support. T.D.Z.A. thanks FAPESP, FINEP, and CNPq (Brazil) for financial support.

References and Notes

- (1) Lakowicz, J. R. *Principles of fluorescence spectroscopy*; Plenum Press: New York, 1986.
- (2) Winnik, M. A. In *Photophysical and Photochemical Tools in Polymer Science: Conformation, Dynamic and Morphology*; NATO ASI Series 182; Winnik, M. A., Ed.; Reidel: Dordrecht, The Netherlands, 1986.
- (3) Morawetz, H. In *New Trends in the Photochemistry of Polymers*; Allen, N. S., Rabek, J. F., Eds.; Elsevier Applied Science: London, 1985.
- (4) Mikos, F.; Morawetz, H.; Dennis, K. S. *Macromolecules* **1984**, *17*, 60.
- (5) Winnik, M. A.; Li, X.; Guillet, J. E. *Macromolecules* **1983**, *16*, 992.
- (6) Bravo, J.; Mendicutti, F.; Saiz, E.; Mattice, W. L. *J. Fluoresc.* **1996**, *6*, 41.
- (7) Salom, C.; Semlyen, J. A.; Clarson, S.; Hernández-Fuentes, I.; Maçanita, A. L.; Horta, A.; Piérola, I. F. *Macromolecules* **1991**, *24*, 6827.
- (8) Shiah, T. Y.-J.; Morawetz, H. *Macromolecules* **1984**, *17*, 792.
- (9) Gonzalez-Benito, J.; Cabanelas, J. C.; Aznar, A.; Vigil, M. R.; Bravo, J.; Baselga, J. *J. Appl. Polym. Sci.* **1996**, *62*, 375.
- (10) Guillet, J. E. In *Photophysical and Photochemical Tools in Polymer Science: Conformation, Dynamic and Morphology*; NATO ASI Series 182; Winnik, M. A., Ed.; Reidel: Dordrecht, The Netherlands, 1986; p 467.
- (11) Talhivini, M.; Atvars, T. D. Z.; Cui, C.; Weiss, R. G. *Polymer* **1996**, *37*, 4365.
- (12) Serrano, B.; Levenfeld, B.; Bravo, J.; Baselga, J. *Polym. Eng. Sci.* **1996**, *36*, 175.
- (13) Pekcan, Ö.; Yilmaz, Y.; Okay, O. *Polymer* **1996**, *37*, 2049.
- (14) Mandelkern, L. *Physical Properties of Polymers*; ACS Professional Reference Book; American Chemical Society: Washington, D.C., 1993; Chapter 4.
- (15) Ohta, Y.; Yasuda, H. *J. Polym. Sci., Part B: Polym. Phys.* **1994**, *32*, 2241.
- (16) Atvars, T. D. Z.; Sabadini, E.; Martim-Franchetti, S. M. *Eur. Polym. J.* **1993**, *29*, 1259.
- (17) Kalyanasundaram, K.; Thomas, J. K. *J. Am. Chem. Soc.* **1977**, *99*, 2039, and references cited therein.
- (18) Michl, J.; Thulstrup, E. W. *Spectroscopy with polarized light*; VCH: New York, 1995.
- (19) Tuan, V. D.; Wild, V. P.; Lamotte, M.; Merle, A. M. *Chem. Phys. Lett.* **1976**, *39*, 119.
- (20) Pellois, A.; Ripoche, J. *Chem. Phys. Lett.* **1969**, *3*, 280.
- (21) Karpovich, D. S.; Blanchard, G. J. *J. Phys. Chem.* **1995**, *99*, 3951.
- (22) Kalyanasundaram, K. *Photochemistry in Microheterogeneous Systems*; Academic Press: Orlando, FL, 1987; p 39.
- (23) Langkilde, F. W.; Thulstrup, E. W.; Michl, J. *J. Chem. Phys.* **1983**, *78*, 3372.
- (24) Birks, J. B. *Photophysics of aromatic molecules*; Wiley Interscience: New York, 1970.
- (25) Becker, R. S. *Theory and Interpretation of Fluorescence and Phosphorescence*; Wiley Interscience: New York, 1968.
- (26) Winnik, F. M. *Chem. Rev.* **1993**, *93*, 587.
- (27) Foggi, P.; Pettini, L.; Santa, I.; Righini, R.; Califano, S. *J. Phys. Chem.* **1995**, *99*, 7439.
- (28) Cyvin, S. J.; Cyvin, B. N.; Brunvoll, J.; Whitmer, J. C.; Klæboe, P.; Gustavsen, J. E. *Z. Naturforsch A* **1979**, *34*, 876.
- (29) Willis, H. A.; Cudby, M. E. In *Structural Studies of Macromolecules by Spectroscopic Methods*; Ivin, K. J., Ed.; Wiley: New York, 1976; Chapter 7.
- (30) Koenig, J. L. *Spectroscopy of Polymers*; American Chemical Society: Washington, D.C., 1991.
- (31) Henderson, B.; Imbusch, G. F. *Optical Spectroscopy of Inorganic Solids*; Oxford University Press: Oxford, U.K., 1989; p 183.
- (32) Bershtein, V. A.; Egorov, V. M. *Differential Scanning Calorimetry of Polymers*; Horwood: Hemmel Hempstead, Great Britain, 1994; p 65.
- (33) Cheng, S. Z. D. *J. Appl. Polym. Sci.: Appl. Polym. Symp.* **1989**, *43*, 315.
- (34) The infrared spectrum of LDPE below and above 273 K shows only slight differences in the frequency range $400\text{--}2700 \text{ cm}^{-1}$, but at low temperatures a broad band centered at 3200 cm^{-1} appears; this band extends to lower energies and is masked by the strong absorption at about 2800 cm^{-1} . At room temperature this broad band disappears.